

Approximate Waveforms for Extreme-Mass-Ratio Inspirals: The Chimera Scheme

Carlos F. Sopuerta¹ and Nicolás Yunes^{2,3,4}

¹Institut de Ciències de l'Espai (CSIC-IIEEC), Facultat de Ciències, Campus UAB, Torre C5 parells, Bellaterra, 08193 Barcelona, Spain.

²Department of Physics, Montana State University, Bozeman, MT 59717, USA.

³Department of Physics and MIT Kavli Institute, 77 Massachusetts Avenue, Cambridge, MA 02139, USA.

⁴Princeton University, Physics Department, Princeton, NJ 08544, USA.

E-mail: sopuerta@ieec.uab.es, nyunes@physics.montana.edu

Abstract. We describe a new kludge scheme to model the dynamics of generic extreme-mass-ratio inspirals (EMRIs; stellar compact objects spiraling into a spinning supermassive black hole) and their gravitational-wave emission. The *Chimera* scheme is a hybrid method that combines tools from different approximation techniques in General Relativity: (i) A multipolar, post-Minkowskian expansion for the far-zone metric perturbation (the gravitational waveforms) and for the local prescription of the self-force; (ii) a post-Newtonian expansion for the computation of the multipole moments in terms of the trajectories; and (iii) a BH perturbation theory expansion when treating the trajectories as a sequence of self-adjusting Kerr geodesics. The EMRI trajectory is made out of Kerr geodesic fragments joined via the method of osculating elements as dictated by the multipolar post-Minkowskian radiation-reaction prescription. We implemented the proper coordinate mapping between Boyer-Lindquist coordinates, associated with the Kerr geodesics, and harmonic coordinates, associated with the multipolar post-Minkowskian decomposition. The Chimera scheme is thus a combination of approximations that can be used to model generic inspirals of systems with extreme to intermediate mass ratios, and hence, it can provide valuable information for future space-based gravitational-wave observatories, like LISA, and even for advanced ground detectors. The local character in time of our multipolar post-Minkowskian self-force makes this scheme amenable to study the possible appearance of transient resonances in generic inspirals.

1. Introduction

The modeling of gravitational wave (GW) sources is key for the success of GW astronomy. Detectors require precise theoretical waveforms to extract and characterize signals buried in the noise. One of the main GW sources for space-based observatories, like the *Laser Interferometer Space Antenna* (LISA) [1, 2], that requires accurate templates for detection and analysis are extreme-mass-ratio inspirals (EMRIs) [3]. These events consist of a small compact object (SCO), such as a stellar-mass black hole (BH) or a neutron star, spiraling in a generic orbit into a spinning, (super)massive black hole (MBH), in the regime where GW emission is relevant. In such inspirals, the SCO spends up to millions of cycles in close orbits around the MBH, possibly with large pericenter velocities and eccentricities, sampling the strong gravitational field of the MBH.

The relevant EMRI phase for data analysis is the inspiral, during which the number of cycles accumulated scales with the inverse of the mass ratio $q = m_*/M_\bullet$ [$\mathcal{O}(10^{-4})$ - $\mathcal{O}(10^{-6})$]. During EMRI plunge and merger, the accumulated number of cycles scales with the MBH mass (M_\bullet) only. Moreover, the signal-to-noise ratio (SNR) is in the range $\mathcal{O}(10)$ - $\mathcal{O}(10^2)$ for EMRIs at realistic distances, and it scales linearly with the total number of cycles. Therefore, the contribution of the merger/plunge phase to the SNR is a fraction $\mathcal{O}(m_*/M_\bullet)$ relative to the total inspiral contribution. In addition, the EMRI ringdown phase is not detectable, as the SCO barely perturbs the MBH geometry as it plunges and crosses the MBH's event horizon.

As a consequence of the large number of GW cycles contained in EMRIs, they can provide a detailed map of the MBH geometry, allowing us to extract the EMRI physical parameters with high precision [4]. This information is crucial to test the Kerr hypothesis [5, 6, 7, 8, 9, 10] and constrain modified gravity theories (see, e.g. [11, 12, 10, 13]). EMRI observations will also have an important impact on astrophysics (for a review see [3]).

The extreme mass ratios involved in the problem also lead to the appearance of two different spatial and temporal scales. The two different spatial scales are due to the different MBH and SCO sizes, $m_*/M_\bullet \ll 1$. The two different temporal scales are the orbital one(s) and the one associated with *radiation reaction*, $T_{\text{Orbital}}/T_{\text{RR}} \sim m_*/M_\bullet \ll 1$. Due to this, a fully relativistic numerical evolution of EMRIs is currently unfeasible.

A framework to model EMRIs that exploits the extreme mass ratios involved is BH perturbation theory, where one treats the SCO as a small perturbation of the MBH background geometry. In this context, the inspiral is modeled as due to a local *self-force*. This force is composed of the metric perturbations generated by the SCO, regularized by eliminating divergences due to the SCO's point particle description. The SCO's motion is then governed by the MiSaTaQuWa equation of motion, derived in [14, 15]. This equation is the foundation of a self-consistent scheme to describe EMRIs in an *adiabatic* way, by coupling this equation of motion to the partial differential equations that describe the perturbations produced by the SCO.

At present, the gravitational self-force has been computed for the case of a non-rotating MBH using time-domain techniques [16, 17]. Progress is currently being made toward the calculation of more astrophysically relevant (spinning) EMRIs [18]. Given the number of cycles contained produced by an EMRI in one year and the present complexity of self-force calculations, we cannot expect to generate complete waveform template banks by means of full self-force calculations. Instead, it has been proposed that the goal of these studies should be to understand all the details of the structure of the self-force, so that one can formulate efficient and precise algorithms (phenomenological models) to create the waveforms needed for LISA data analysis, perhaps complementing existent approximation schemes.

In this paper, we summarize the results of [19] where a new *approximate* scheme was proposed to model EMRIs: the Chimera framework. This scheme can be thought of as a new *kludge* model that combines different approximation methods, including BH perturbation theory, the multipolar post-Minkowskian formalism of Blanchet and Damour [20] and post-Newtonian theory. The Chimera scheme could be used for qualitative descopeing studies, i.e. to determine the accuracy to which parameters could be extracted given an eLISA EMRI detection as a function of detector properties. The Chimera scheme could also be used to study how certain resonances, found by Flanagan and Hinderer [21], affect such parameter estimation and detection. Chimera waveforms, however, would require improvements before they can be used as realistic templates in data analysis. The Chimera scheme is indeed amenable to such improvements, which will be the focus of future work.

2. Ingredients of the Chimera Scheme

2.1. MBH Geometry and Geodesic Motion

The geometry of the MBH is described by the Kerr metric. In Boyer-Lindquist (BL) coordinates, $(x_{\text{BL}}^\mu) = (t, r, \theta, \phi)$, the line element is given by

$$ds^2 = -dt^2 + \frac{\rho^2}{\Delta} dr^2 + \rho^2 d\theta^2 + (r^2 + a^2) \sin^2 \theta d\phi^2 + \frac{2M_\bullet r}{\rho^2} (dt - a \sin^2 \theta d\phi)^2, \quad (1)$$

where $\rho^2 = r^2 + a^2 \cos^2 \theta$ and $\Delta = r^2 - 2M_\bullet r + a^2 = r^2 f + a^2$, with $f = 1 - 2M_\bullet/r$. The function Δ has two roots: $r_\pm \equiv M_\bullet \pm \sqrt{M_\bullet^2 - a^2}$; the positive one r_+ ($\geq r_-$) coincides with the location of the event horizon. The Kerr geometry is a stationary, axisymmetric and vacuum solution to the Einstein equations, which has an additional symmetry described by a Killing tensor.

In the limit where the SCO has zero mass ($m_* \rightarrow 0$), it follows timelike geodesics of the MBH geometry which, in terms of proper time, can be parameterized as $z^\mu(\tau) = (t(\tau), r(\tau), \theta(\tau), \phi(\tau))$. Given the symmetries of the Kerr metric, each of these geodesics can be fully characterized by three constants of motion (per SCO unit mass): The energy (stationarity), E ; the angular momentum in the MBH spin direction (axisymmetry), L_z , and the *Carter constant* (Killing tensor symmetry), Q (or $C \equiv Q - (L_z - aE)^2$). Using these symmetries we can completely separate the geodesic equations so that they can be written in the form:

$$\rho^2 \frac{dt}{d\tau} = \frac{1}{\Delta} (\Sigma^2 E - 2M_\bullet a r L_z), \quad (2)$$

$$\rho^4 \left(\frac{dr}{d\tau} \right)^2 = [(r^2 + a^2) E - a L_z]^2 - (Q + r^2) \Delta, \quad (3)$$

$$\rho^4 \left(\frac{d\theta}{d\tau} \right)^2 = C - \cot^2 \theta L_z^2 - a^2 \cos^2 \theta (1 - E^2), \quad (4)$$

$$\rho^2 \frac{d\phi}{d\tau} = \frac{1}{\Delta} \left[2M_\bullet a r E + \frac{L_z}{\sin^2 \theta} (\Delta - a^2 \sin^2 \theta) \right], \quad (5)$$

where $\Sigma^2 \equiv (r^2 + a^2)^2 - a^2 \Delta \sin^2 \theta$. For the purposes of EMRI modeling we restrict ourselves to bound geodesics (orbits), which can also be characterized in terms of orbital elements: the eccentricity e , the semilatus rectum p , and the inclination θ_{inc} . The first two are defined in terms of the turning points (extrema) of the radial motion, the pericenter and apocenter (r_{peri} and r_{apo}), by the Newtonian relations: $r_{\text{peri}} = pM_\bullet/(1+e)$ and $r_{\text{apo}} = pM_\bullet/(1-e)$. Likewise, the inclination angle θ_{inc} is associated with the turning point of the polar motion, i.e. the minimum of θ ($\theta_{\text{min}} \in [0, \pi/2]$), via the relation: $\theta_{\text{inc}} = \text{sign}(L_z) (\pi/2 - \theta_{\text{min}})$. Another useful definition of the orbital inclination angle is: $\cos \iota = L_z / \sqrt{L_z^2 + C}$.

Alternatively, the orbits can also be characterized in terms of three *fundamental* frequencies (see e.g. [22, 23, 24]) with respect to the BL time t (they can be also constructed using proper time or any other time): Ω_r , associated with the radial motion (from periapsis to apoapsis and back); Ω_θ , associated with polar motion; and Ω_ϕ , associated with azimuthal motion. Precessional orbital effects are due to mismatches between these frequencies, and they can be used to decompose, among other things, the GWs in a Fourier expansion [23].

2.2. Chimera Osculating Trajectories

The foundations of the gravitational backreaction of a moving massive body on its own trajectory were laid down in the papers by Mino, Tanaka, and Sasaki [14] and Quinn and Wald [15]. These works established that the trajectory of a point mass can be understood as geodesic motion in the background geometry modified by a local force, the *self-force*, given in terms of the gradients

of the *regularized*¹ first-order metric perturbations. Then, the equation of motion for the SCO, the MiSaTaQuWa equation, is

$$\frac{d^2 z^\alpha}{d\tau^2} + \Gamma_{\mu\nu}^\alpha u^\mu u^\nu = m_\star^{-1} F_{\text{SF}}^\alpha, \quad (6)$$

where the self-force, F_{SF}^α , is given by

$$F_{\text{SF}}^\alpha = -\frac{1}{2} m_\star \left(g^{\alpha\lambda} + u^\alpha u^\lambda \right) u^\mu u^\nu \left(2\nabla_\mu h_{\nu\lambda}^{\text{R}} - \nabla_\lambda h_{\mu\nu}^{\text{R}} \right), \quad (7)$$

and $h_{\mu\nu}^{\text{R}}$ denotes the regularized metric perturbations. This equation can be also reinterpreted as a geodesic equation for a point particle in the perturbed geometry $g_{\alpha\beta} + h_{\alpha\beta}^{\text{R}}$ [26]. In order to evolve the SCO's trajectory subject to the self-force in a self-consistent way, we use the method proposed in [27], which is a relativistic extension of the *osculating orbit method*. The main idea is to model the SCO's worldline as a sequence of geodesics tangent to the worldline at any given point. The transition is smooth since EMRI trajectories remain close to a geodesic for a significant amount of time. In principle, to carry out this transition we need to take into account all the parameters that characterize the *instantaneous* geodesic (the *principal* orbital elements) and the position of the SCO within that geodesic (the *positional* orbital elements). In the initial version of the Chimera scheme [19] we only consider the dissipative effects of the self-force, i.e. those that only affect to principal orbital elements. Then, the evolution of $(E, L_z, C/Q)$ is given by

$$\frac{dE}{d\tau} = -\zeta_\alpha^{(t)} a_{\text{SF}}^\alpha, \quad \frac{dL_z}{d\tau} = \zeta_\alpha^{(\phi)} a_{\text{SF}}^\alpha, \quad (8)$$

$$\frac{dQ}{d\tau} = 2 \xi_{\alpha\beta} u^\alpha a_{\text{SF}}^\beta, \quad \frac{dC}{d\tau} = \frac{dQ}{d\tau} + 2(aE - L_z) \left(\frac{dL_z}{d\tau} - a \frac{dE}{d\tau} \right), \quad (9)$$

where the SCO self-acceleration a_{SF}^α is related to the self-force by $a_{\text{SF}}^\alpha = m_\star^{-1} F_{\text{SF}}^\alpha$, and where $\zeta_\alpha^{(t)}$ and $\zeta_\alpha^{(\phi)}$ are the timelike and axial Killing vectors respectively, and $\xi_{\alpha\beta}$ is the Killing tensor.

2.3. Multipolar Post-Minkowskian Self-Acceleration

Since the self-force is not known for generic Kerr orbits, we approximate it here via a multipolar, post-Minkowskian expansion (see e.g. [20, 28, 29]). We begin by recasting the post-Minkowskian metric perturbation in the far field as the Kerr metric of the MBH $g_{\mu\nu}^{\text{K,H}}$ in harmonic coordinates (we shall discuss the issue of coordinates in next section), plus perturbations induced by the SCO. The latter can be decomposed into conservative (*time-symmetric*) and dissipative (*time-asymmetric*) perturbations $h_{\mu\nu}^{\text{RR}}$. Neglecting the former, we then have

$$g_{\mu\nu}^{\text{PM}} = g_{\mu\nu}^{\text{K,H}} + h_{\mu\nu}^{\text{RR}}, \quad (10)$$

The metric perturbations $h_{\mu\nu}^{\text{RR}}$ are the quantities we use to describe the *radiation-reaction* effects, and hence they are our approximation to the regularized metric perturbations $h_{\alpha\beta}^{\text{R}}$ of Eqs. (6) and (7). The rate of change of the principal orbital elements is then described by Eq. (8), with the force of Eq. (7) and the regularized metric perturbation of Eq. (10).

The regular metric perturbation is a function of certain time-asymmetric scalar, V_{RR} , and vector, V_{RR}^i , radiation-reaction potentials, which to lowest order can be written as

$$h_{tt}^{\text{RR}} = 2 V_{\text{RR}}, \quad h_{ti}^{\text{RR}} = -4 V_{\text{RR}}^i, \quad h_{ij}^{\text{RR}} = 2 V_{\text{RR}} \delta_{ij}, \quad (11)$$

¹ For a point mass, the first-order metric perturbation is singular at the particle location, and a regularization prescription [25] must be employed to separate out the piece responsible of the gravitational backreaction.

and the expressions for these potentials themselves are [20, 30]

$$V_{\text{RR}}(t_{\text{H}}, \mathbf{x}_{\text{H}}) = -\frac{1}{5}x_{\text{H}}^{ij}M_{ij}^{(5)}(t_{\text{H}}) + \frac{1}{189}x_{\text{H}}^{ijk}M_{ijk}^{(7)}(t_{\text{H}}) - \frac{1}{70}\mathbf{x}_{\text{H}}^2x_{\text{H}}^{ij}M_{ij}^{(7)}(t_{\text{H}}) + \mathcal{O}(x_{\text{H}}^iM_{ij}^{(9)}), \quad (12)$$

$$V_{\text{RR}}^i(t_{\text{H}}, \mathbf{x}_{\text{H}}) = \frac{1}{21}x_{\text{H}}^{<ijk>}M_{jk}^{(6)}(t_{\text{H}}) - \frac{4}{45}\epsilon_{ijk}x_{\text{H}}^{jl}S_{kl}^{(5)}(t_{\text{H}}) + \mathcal{O}(x_{\text{H}}^{ijk}M_{ij}^{(8)}), \quad (13)$$

where $(x_{\text{H}}^{\alpha}) = (t_{\text{H}}, x_{\text{H}}^i)$ are spacetime harmonic coordinates, ϵ_{ijk} is the antisymmetric Levi-Civita symbol, and

$$\hat{x}_{\text{H}}^{<ijk>} \equiv x_{\text{H}}^{ijk} - \frac{3}{5}\mathbf{x}_{\text{H}}^2\delta^{(ij}x_{\text{H}}^{k)}. \quad (14)$$

is the symmetric trace-free (STF) projection of the multi-index quantity $x^{ijk} = x^ix^jx^k$. The quantities $M_{ij}^{(n)}$, $M_{ijk}^{(n)}$, and $S_{ij}^{(n)}$ are the n th-time-derivative of the STF mass quadrupole, mass octopole and current quadrupole multipole moments of the source. The first term in V_{RR} [Eq. (12)] corresponds to the well-known Burke-Thorne radiation reaction potential [31].

The Chimera local self-force is completely specified once we prescribe how the multipole moments depend on the orbital trajectories. This can be achieved by asymptotically matching a PN and a post-Minkowskian solution in some buffer zone where both approximations are valid. The current Chimera implementation employs the leading-order expressions for these multipoles. As such, we are not consistently keeping a given PN order, but instead using leading-order expressions for the multipole moments, while keeping several such moments in the expansions. To lowest order, the mass moments are given by

$$M_{ij} = \eta m z_{<ij>}, \quad M_{ijk} = \eta \delta m z_{<ijk>} \quad (15)$$

and the current quadrupole moment is

$$S_{ij} = \eta \delta m \epsilon_{kl<i}z_{j>}^k \dot{z}^l, \quad (16)$$

where $\eta = m_{\star}M_{\bullet}/(m_{\star} + M_{\bullet})^2$ is the symmetric mass ratio and $\delta m = M_{\bullet} - m_{\star}$ is the mass difference. To higher order, these moments become more complicated as there are now non-linear contributions from the non-reactive potentials (i.e. non-linear contributions from the background) as well as tail and memory contributions.

2.4. From Boyer-Lindquist to Harmonic Coordinates

From the previous discussion it is clear that the MBH metric must be written in harmonic coordinates in order for all terms to be in the same coordinate system and to be consistent with other ingredients of the Chimera scheme, in particular the waveform generation procedure that we describe in next section. Nevertheless, there are parts of the scheme that are easier to implement in BL coordinates, such as the integration of the geodesic equations. Therefore, it is crucial to find a map from BL to harmonic coordinates.

Harmonic coordinates refer to coordinate systems, $\{x_{\text{H}}^{\alpha}\}$, that satisfy $\square x_{\text{H}}^{\alpha} = 0$, where \square is the D'Alembertian operator: $\square \equiv g^{\alpha\beta}\nabla_{\alpha}\nabla_{\beta}$. In [32], based on work by Ding (see Ref. [32] for references on this), a transformation to harmonic coordinates was found. Following [32], we can map the Kerr metric from BL coordinates (t, r, θ, ϕ) to harmonic ones $(t_{\text{H}}, x_{\text{H}}, y_{\text{H}}, z_{\text{H}})$, and the

converse, via the coordinate transformations

$$\begin{aligned}
t_{\text{H}} &= t, & t &= t_{\text{H}}, \\
x_{\text{H}} &= \sqrt{(r - M_{\bullet})^2 + a^2} \sin \theta \cos[\phi - \Phi(r)], & r &= M_{\bullet} + \left[\frac{r_{\text{H}}^2 - a^2}{2} + \sqrt{\left(\frac{r_{\text{H}}^2 - a^2}{2}\right)^2 + a^2 z_{\text{H}}^2} \right]^{1/2}, \\
y_{\text{H}} &= \sqrt{(r - M_{\bullet})^2 + a^2} \sin \theta \sin[\phi - \Phi(r)], & \theta &= \arccos\left(\frac{z_{\text{H}}}{r - M_{\bullet}}\right), \\
z_{\text{H}} &= (r - M_{\bullet}) \cos \theta, & \phi &= \Phi(r) + \arctan\left(\frac{y_{\text{H}}}{x_{\text{H}}}\right),
\end{aligned} \tag{17}$$

where $r_{\text{H}} \equiv (x_{\text{H}}^2 + y_{\text{H}}^2 + z_{\text{H}}^2)^{1/2}$ and the angle function $\Phi(r)$ is given by

$$\Phi(r) = \frac{\pi}{2} - \arctan\left\{ \frac{\frac{r - M_{\bullet}}{a} + \Omega(r)}{1 - \frac{r - M_{\bullet}}{a} \Omega(r)} \right\}, \quad \text{with } \Omega(r) = \tan\left[\frac{a}{2\sqrt{M_{\bullet}^2 - a^2}} \ln\left(\frac{r - r_-}{r - r_+}\right) \right]. \tag{18}$$

2.5. Waveform Generation

Given the orbital evolution in harmonic coordinates one can construct the gravitational waveforms through multipolar, post-Minkowskian expressions in terms of a sum over multipole moments (see e.g. [33] for a review). This prescription is fully specified once expressions for the radiative moments are given in terms of derivatives of the orbital trajectory. Such identification, however, is difficult, as these moments are defined in the *far-zone* and have no knowledge of the *source* multipole moments, defined in the *near zone*. In this initial version of the Chimera scheme, we only consider the leading-order contributions to the multipoles moments, i.e. we identify the source and radiative moments. Then, in a transverse-traceless gauge and keeping multipole moments that include both the mass hexadecapole and the current octopole (thus keeping contributions one order higher than traditional kludge waveforms), we have:

$$h_{ij}^{\text{TT}} = \frac{2}{r} \ddot{M}_{ij}^{\text{STF}} + \frac{2}{3r} \left[\ddot{M}_{ijk} n^k + 4\epsilon^{kl} ({}_i\ddot{S}_j)_k n_l \right]^{\text{STF}} + \frac{1}{6r} \left[\ddot{M}_{ijkl} n^k n^l + 6\epsilon^{kl} ({}_i\ddot{S}_j)_{km} n^l n^m \right]^{\text{STF}}. \tag{19}$$

The expressions for these multipole moments has been given in Eqs. (15) and (16), except for the mass hexadecapole and current octopole multipoles, which are given respectively by

$$M_{ijkl} = \eta m z_{\langle ijkl \rangle}, \quad S_{ijk} = \eta m \epsilon_{lm \langle i} z_{jk \rangle}^l z^m. \tag{20}$$

The plus and cross-polarized projections can then be constructed via

$$h_{+, \times} = e_{+, \times}^{ij} h_{ij}^{\text{TT}}, \tag{21}$$

where $e_{+, \times}^{ij}$ are the plus- and cross-polarization tensors. Finally, the observables, i.e. the GW response function, are given by a projection of the plus- and cross-polarized waveform with the beam pattern functions of the detector. For a detector like LISA, there are two such functions, $F_{+, I/II}$ and $F_{\times, I/II}$ (see, e.g. [34, 4]) and the response is thus

$$h \equiv \frac{\sqrt{3}}{2 D_L} \sum_{A=I, II} (F_{+, A} h_+ + F_{\times, A} h_{\times}), \tag{22}$$

where D_L is the luminosity distance from the source to the observer and the prefactor of $\sqrt{3}/2$ is due to the triangular arrangement of the LISA spacecraft constellation.

3. Numerical Implementation and some Numerical Results

One of the main ingredients of the scheme is the integration of the geodesic equations (2)-(5). The resulting equations for the radial and polar BL coordinates, Eqs. (3) and (4) respectively, have turning points (at pericenter and apocenter in the case of the radial coordinate, and at the location of the orbital inclination angle in the case of the polar coordinate). At these points we have either $\dot{r} = 0$ or $\dot{\theta} = 0$ and the ODE solvers may encounter convergence problems. To avoid these problems, we use angle variables associated with radial and polar BL coordinates via

$$r = \frac{pM_{\bullet}}{1 + e \cos \psi}, \quad \cos^2 \theta = \cos^2 \theta_{\min} \cos^2 \chi. \quad (23)$$

For convenience, we parametrize the trajectory in terms of the BL coordinate time t , which is also a time harmonic coordinate, instead of the proper time τ . Then, the direct result of the ODE integration is the sequence $(t, \psi(t), \chi(t), \phi(t))$ for $t \in [t_{\text{ini}}, t_{\text{end}}]$.

The main challenge in the numerical implementation of the Chimera scheme is the evaluation of the time derivatives of the different quantities involved. To understand this problem let us focus on the computation of our multipolar, post-Minkowskian self-force. The radiation reaction potentials V_{RR} and V_{RR}^i in (12) and (13) depend on up to the seventh time derivative of the mass quadrupole and octopole moments and up to the fifth time derivative of the current quadrupole moment. But since one also needs certain time derivatives of these potentials [see Eq. (7)] one must compute up to the eighth time derivative of the mass quadrupole and octopole moments and the sixth time derivative of the current quadrupole moment.

In principle, the computation of these derivatives can be done analytically by using repeatedly the equations of motion, Eqs. (2)-(5). The problem is that we need the time derivatives of the trajectory in harmonic coordinates, and to pass from the ODE angles $(\psi(t), \chi(t), \phi(t))$ to harmonic coordinates we first need to use Eq. (23) to go from these angles to BL coordinates, and then Eqs. (17) to go from BL to harmonic coordinates. Therefore, we would need to obtain analytically higher time-derivatives of the ODE angles (up to eighth order), which involves using Christoffel symbols of the Kerr metric and several of their derivatives, and also to differentiate several times Eqs. (23) and (17). In practice, this makes the analytical computations unfeasible, even using modern computer algebra systems.

Therefore, one needs to resort to numerical evaluations of these derivatives. First, notice that the trajectory, the velocity, and the acceleration can be computed with high accuracy directly from the integration of the ODEs in Eqs. (2)-(5). Then, using analytical expressions, we can directly obtain the second time derivatives of the mass quadrupole and octopole moments and the first time derivative of the current quadrupole moment. Thus, we just need to compute numerically up to six additional time derivative of the mass moments (i.e. starting from their second time derivative) and up to five additional time derivative of the current quadrupole moment (i.e. starting from its first time derivative).

Computing numerical derivatives is a subtle task, which we tried to implement in different ways. For instance, we experimented with many finite difference rules (involving from a few to more than 20 evaluation points), as well as other generic numerical differentiation techniques (such as numerical interpolation or Chebyshev differentiation). We found that, in order to obtain decent performance, a substantial amount of fine-tuning was necessary. To overcome this difficulty, we looked for a method better adapted to our problem. Notice that multipole moments are functionals of the trajectories, which are piecewise Kerr bounded geodesic, and bounded geodesics can be characterized by three fundamental frequencies (in the generic case). Then, an arbitrary functional of Kerr orbits, say $f[\psi, \chi, \phi](t)$, can be expanded in a multiple Fourier series of these frequencies as [23]

$$f[\psi, \chi, \phi](t) = \sum_{k,m,n} f_{k,m,n} e^{-i(k\Omega_r + m\Omega_{\theta} + n\Omega_{\phi})t}, \quad (24)$$

where (k, m, n) are integers running from $-\infty$ to $+\infty$ and $f_{k,m,n}$ are complex coefficients such that $f_{-k,-m,-n} = \bar{f}_{k,m,n}$. There are three special cases in which this expansion is simplified: (i) Circular equatorial orbits; (ii) Equatorial non-circular orbits; (iii) Circular non-equatorial orbits. In case (i), the Fourier series contains only a single frequency, the azimuthal one Ω_ϕ . In case (ii) and (iii), there are two independent frequencies, (Ω_r, Ω_ϕ) and $(\Omega_\theta, \Omega_\phi)$ respectively.

By modeling the required multipole moments as an expansion of the form of Eq. (24), using a standard least-square fitting algorithm, time derivatives are then computed via

$$f^{(N)}[\psi, \chi, \phi](t) = \sum_{k,m,n} f_{k,m,n}^N e^{-i(k\Omega_r + m\Omega_\theta + n\Omega_\phi)t}, \quad (25)$$

where $f_{k,m,n}^N = (-i)^N (k\Omega_r + m\Omega_\theta + n\Omega_\phi)^N f_{k,m,n}$. We tested this technique with different types of functions and we have found that it is very robust and provides very high accuracy even for the highest derivatives. For instance, the sixth time derivative is typically accurate to one part in 10^5 , which is more than enough for our purposes.

In order to illustrate the strengths of the Chimera scheme, we present results for a generic, eccentric and inclined orbit. The evolution of all the constants of motion/orbital elements for many orbital periods is shown in Figure. 1. While the large scale evolution looks very smooth, the shorter scale evolution in the subplots shows patterns with periods that match the orbital ones. These patterns are a consequence of using a local in time self-force and do not appear in evolutionary schemes based on flux averaging over a certain number of orbital periods. We can also appreciate from the global evolution that all quantities decay in time except for the inclination, which grows. However, if we look at the evolution over a few orbital periods, e.g. for the eccentricity, we can see that it can grow locally in time although the global tendency is to decay. The Chimera scheme leads to rich evolutionary patterns due to its local-in-time character, which also makes it a very valuable tool to investigate questions like transient resonances [21].

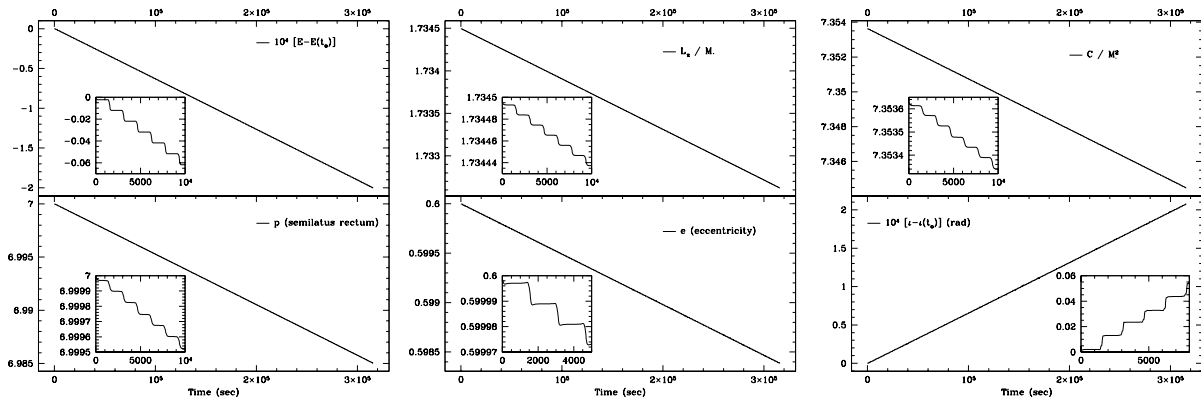


Figure 1. Evolution (for a total time of 10^{-2} yrs) of an eccentric and inclined inspiral of a system characterized by: $M_\bullet = 10^6 M_\odot$, $a/M_\bullet = 0.98$, and $q = 10^{-5}$. The plots show the evolution of the following quantities: Energy E (top left), actually $10^4[E - E(t_0)]$, where $E(t_0) = 0.9575513$; angular momentum along the spin axis, L_z (top centre); Carter constant C (top right); semi-latus rectum, p (bottom left), with $p(t_0) = 7$; eccentricity, e (bottom centre), with $e(t_0) = 0.6$; and inclination angle ι (bottom right), actually $10^4[\iota - \iota(t_0)]$, where $\iota(t_0) = 57.39$ deg. All plots contain subplots where the detailed evolution during a few orbital periods is shown.

4. Conclusions and Discussion

We have presented the main ingredients of the Chimera scheme, a framework initially designed for the modeling of EMRI dynamics and GW emission, but in principle also adaptable to intermediate-mass ratio systems. This scheme combines ingredients from the multipolar, post-Minkowskian formalism and black hole perturbation theory to evolve a non-geodesic worldline (with respect to the MBH geometry) and to construct waveforms. The orbits are built as a sequence of local geodesics, whose orbital elements evolve according to a local self-force that we approximate via a multipolar, post-Minkowskian expansion. The leading-order term of the self-force corresponds to the well-known Burke-Thorne radiation-reaction potential. A crucial ingredient in this construction is the mapping from BL coordinates, which we use to locally integrate the orbits, to harmonic coordinates, required both by the multipolar, post-Minkowskian self-force and by the GW multipolar expansion. Once we have trajectories in harmonic coordinates, it is straightforward to build waveforms.

The Chimera scheme can be improved in different ways. One possibility is to use more accurate, beyond leading-order, expressions for the different multipole moments. Although these PN corrections are in general not known for generic spinning binaries, they should certainly improve the accuracy of the Chimera evolutions for certain orbits. Another way to improve the scheme would be to introduce conservative corrections to the background, for instance as it is done in the EOB formalism [35, 36, 37].

A more detailed and exhaustive validation of the Chimera scheme would include, as a first step, a comparison of the evolution of the constants of motion with those obtained by solving the Teukolsky equation [38, 39]. One has to be careful in doing this comparison given that the latter employs averages over several cycles, while the Chimera fluxes are computed locally at the SCO's location. Once the fluxes have been validated, one should compare the waveforms themselves. An overlap study would determine the level of agreement between them.

The Chimera scheme might also be useful to model IMRIs and even systems with moderate mass ratios. Recent comparisons between self-force, PN, and numerical relativity computations have concluded that by replacing the mass ratio q with the symmetric mass ratio η , the self-force predictions compare quite well with numerical relativity and PN predictions in the comparable-mass range [40, 41]. These results may allow for a simpler description of IMRIs, which otherwise would require either long, full numerical computations or higher-order perturbative computations, or a combination of both. In the Chimera scheme, $q \rightarrow \eta$ is actually mostly built in already, since the mass ratio information enters through the definition of the multipole moments. For these, we already use general binary expressions, instead of effective one-body ones with mass qM_\bullet .

The ability to compute approximate local quantities at the location of the SCO, in particular the multipolar, post-Minkowskian self-force, makes the Chimera scheme an interesting tool to study certain local behavior believed to exist in EMRIs. For example, Flanagan and Hinderer [21] have recently reported that certain rapid changes in orbital elements can arise for generic EMRIs when the orbital frequencies become commensurate. During these rapid changes, it has been suggested that EMRI waveforms may present *glitches*. Reliable quantitative predictions for these glitches are needed to assess the importance of this effect for gravitational wave astronomy. In this sense, we could compare the effect of these glitches in waveforms as computed from an averaged-scheme (such as the Teukolsky one) and a local one (such as the Chimera scheme).

Acknowledgments

CFS acknowledges support from the Ramón y Cajal Programme of the Spanish Ministry of Education and Science, by a Marie Curie International Reintegration Grant (MIRG-CT-2007-205005/PHY) within the 7th European Community Framework Programme, and from contract AYA-2010-15709 of the Spanish Ministry of Science and Innovation. NY acknowledges support

from NSF grant PHY-1114374, as well as support provided by the National Aeronautics and Space Administration through Einstein Postdoctoral Fellowship Award Number PF0-110080, issued by the Chandra X-ray Observatory Center, which is operated by the Smithsonian Astrophysical Observatory for and on behalf of the National Aeronautics Space Administration under contract NAS8-03060. NY also acknowledges support from NASA grant NNX11AI49G, under sub-award 00001944. We acknowledge the computational resources provided by the Barcelona Supercomputing Centre (AECT-2011-3-0007) and CESGA (CESGA-ICTS-200).

References

- [1] Danzmann K and Rudiger A 2003 *Class. Quant. Grav.* **20** S1–S9
- [2] Prince T 2003 *American Astronomical Society Meeting* **202** 3701
- [3] Amaro-Seoane P *et al.* 2007 *Class. Quant. Grav.* **24** R113–R169 (*Preprint astro-ph/0703495*)
- [4] Barack L and Cutler C 2004 *Phys. Rev.* **69** 082005 (*Preprint gr-qc/0310125*)
- [5] Collins N A and Hughes S A 2004 *Phys. Rev.* **D69** 124022 (*Preprint gr-qc/0402063*)
- [6] Glampedakis K and Babak S 2006 *Class. Quant. Grav.* **23** 4167–4188 (*Preprint gr-qc/0510057*)
- [7] Barack L and Cutler C 2007 *Phys. Rev.* **D75** 042003 (*Preprint gr-qc/0612029*)
- [8] Vigeland S J and Hughes S A 2010 *Phys. Rev.* **D81** 024030 (*Preprint 0911.1756*)
- [9] Hughes S A 2010 (*Preprint 1002.2591*)
- [10] Sopuerta C F 2010 *Gravitational Wave Notes* **4**(4) 3–47 (*Preprint 1009.1402*)
- [11] Hughes S A 2006 *AIP Conf. Proc.* **873** 233–240 (*Preprint gr-qc/0608140*)
- [12] Schutz B F 2009 *Class. Quant. Grav.* **26** 094020
- [13] Babak S, Gair J R, Petiteau A and Sesana A 2011 *Class. Quant. Grav.* **28** 114001 (*Preprint 1011.2062*)
- [14] Mino Y, Sasaki M and Tanaka T 1997 *Phys. Rev.* **D55** 3457–3476 (*Preprint gr-qc/9606018*)
- [15] Quinn T C and Wald R M 1997 *Phys. Rev.* **D56** 3381–3394 (*Preprint gr-qc/9610053*)
- [16] Barack L and Sago N 2009 *Phys. Rev. Lett.* **102** 191101 (*Preprint 0902.0573*)
- [17] Barack L and Sago N 2010 *Phys. Rev.* **D81** 084021 (*Preprint 1002.2386*)
- [18] Shah A G, Keidl T S, Friedman J L, Kim D H and Price L R 2011 *Phys. Rev.* **D83** 064018 (*Preprint 1009.4876*)
- [19] Sopuerta C F and Yunes N 2011 *Phys. Rev.* **D84** 124060 (*Preprint 1109.0572*)
- [20] Blanchet L and Damour T 1984 *Phys. Lett.* **A104** 82–86
- [21] Flanagan E E and Hinderer T 2010 (*Preprint 1009.4923*)
- [22] Schmidt W 2002 *Class. Quant. Grav.* **19** 2743 (*Preprint gr-qc/0202090*)
- [23] Drasco S and Hughes S A 2004 *Phys. Rev.* **D69** 044015 (*Preprint astro-ph/0308479*)
- [24] Fujita R and Hikida W 2009 *Class. Quant. Grav.* **26** 135002 (*Preprint 0906.1420*)
- [25] Detweiler S and Whiting B F 2003 *Phys. Rev.* **D67** 024025 (*Preprint gr-qc/0202086*)
- [26] Detweiler S 2001 *Phys. Rev. Lett.* **86** 1931–1934 (*Preprint gr-qc/0011039*)
- [27] Pound A and Poisson E 2008 *Phys. Rev.* **D77** 044013 (*Preprint 0708.3033*)
- [28] Iyer B R and Will C M 1993 *Phys. Rev. Lett.* **70** 113–116
- [29] Iyer B R and Will C M 1995 *Phys. Rev.* **D52** 6882–6893
- [30] Blanchet L 1997 *Phys. Rev.* **D55** 714–732 (*Preprint gr-qc/9609049*)
- [31] Burke W L 1971 *J. Math. Phys.* **12** 401–418
- [32] Abe M, Ichinose S and Nakanishi N 1987 *Progress of Theoretical Physics* **78** 1186–1201
- [33] Blanchet L 2006 *Living Rev. Relativity* **9** 4 (*Preprint gr-qc/0202016*)
- [34] Cutler C 1998 *Phys. Rev.* **D57** 7089–7102
- [35] Buonanno A and Damour T 1999 *Phys. Rev.* **D59** 084006 (*Preprint gr-qc/9811091*)
- [36] Buonanno A and Damour T 2000 *Phys. Rev.* **D62** 064015 (*Preprint gr-qc/0001013*)
- [37] Damour T 2010 *Phys. Rev.* **D81** 024017 (*Preprint 0910.5533*)
- [38] Hughes S A 2000 *Phys. Rev.* **D61** 084004
- [39] Hughes S A 2001 *Phys. Rev.* **D64** 064004
- [40] Barack L, Damour T and Sago N 2010 *Phys. Rev.* **D82** 084036 (*Preprint 1008.0935*)
- [41] Le Tiec A, Mrue A H, Barack L, Buonanno A, Pfeiffer H P *et al.* 2011 *Phys. Rev. Lett.* **107** 141101 (*Preprint 1106.3278*)